Effect of CD20 Ca^{2+} channel activity on the efficacy of rituximab and obinutuzumab

Woon Heo

Department of Medical Science

The Graduate School, Yonsei University

Effect of CD20 Ca^{2+} channel activity on the Efficacy of rituximab and obinutuzumab

Directed by Professor Joo Young Kim

The Master's Thesis
submitted to the Department of,
The Graduate School of Yonsei University
in partial fulfillment of the requirements for the degree of
Master of Medical Science

Woon Heo

December 2016

This certifies that The Master's Thesis of Woon Heo is approved.

Thesis Supervisor: Joo Young Kim

Thesis Committee Member #1: Dong Min Shin

Thesis Committee Member #2: Jinu Lee

The Graduate School

Yonsei University

December 2016

ACKNOWLEDGEMENTS

가장 먼저, 제가 약리학교실에 있는 동안 많은 가르침을 주신 김주영 교수님께 감사 드립니다. 교수님의 세심한 조언과 지도 덕분에 제가 발전하는 시간을 가질 수 있었습니다. 또한 김경환 교수님, 안영수 교수님, 이민구 교수님, 박경수 교수님, 김철훈 교수님, 김형범 교수님, 지헌영 교수님께도 감사 드립니다. 교수님들의 가르침이 녹아 있는 약리학 교실에서 수학할 수 있어 영광이었습니다. 학위 논문만이 아니라 실험에도, 또한 실험자의 마음가짐에 대해서도 가르침을 주신 이진우 교수님, 바쁘신 와중에도 제가 놓친 것들을 일깨워 부족한 점을 채울 수 있도록 도와주신 신동민 교수님께 깊이 감사 드립니다.

지난 3년여 간 많은 분들의 도움을 받았습니다. 언제나 바른 소리로 실험실 분위기를 다독거리시는 김연정 선생님, 정남 누나, 그리고 마치 자신의 일처럼 조언을 아끼지 않으신 신동훈 선생님 감사합니다. 힘들어 할 때, 조용히 하지만 큰 힘으로 응원해주신 익현 형, 신혜 누나, 늘 노력하는 모습을 보여주신 지윤 형, 학이 누나, 그리고 한 파트를 책임지며 어깨가 무거울 경지, 장난끼 많지만 분위기메이커 역할을 하는 영익이, 세영이 든든한 버팀목처럼 믿음직한 준석 형 고맙습니다. 활짝 웃는 모습이 좋은 지은 선생님과 혜지 선생님, 저를 살찌우며 보살펴주신 소원 누나 덕분에 제 실험실 자리가 언제나 즐거웠습니다. 지금 실험실에 없지만 저의 정신적 지주가 되어 자리잡도록 도와준 우영 누나, 실험을 알려준 혜민 누나, 정우 형, 지연이, 다시 병원으로 돌아가 환자를 위해 힘쓰고 있는 형순 형, 은석 형, 진세 형, 그리고 제가 장래에 대해 깊이 생각해 보도록 배려해주신 수민 누나, 한상 형, 준희 누나에게도 이렇게나마 지면으로 감사하다고 전해 드립니다.

마지막으로 사랑하는 가족과 제 친우들, 일일이 언급하지 못한 사람들께 고개 숙여 인사 드립니다. 저는 진심으로, 이 시간과 관계를 소중히 간직하겠습니다. 어쩌면 제가 지닌 3년여 간 얻은 것들은 이 페이지에 다 적혀 있을는지 모르겠습니다. 여러분들께도, 그리고 제게도 이따금 찾아올 행운과 값진 노력으로 찾아낼 일상의 행복을 바라겠습니다. 감사합니다.

TABLE OF CONTENTS

LIST OF FIGURES

ABSTRACT

Effect of CD20 channel activity on the efficacy of rituximab and obinutuzumab

Woon Heo

Department of Medical Science
The Graduate School, Yonsei University

(Directed by Professor Joo Young Kim)

CD20 is the first member of four transmembrane spanning family (MS4A) protein, and is a target protein for the rituximab, a monoclonal antibody for the treatment of non-Hodgkin lymphoma and chronic arthritis. Although several previous studies have reported that CD20 function as a Ca^{2+} channels, especially activated by store depletion, the molecular mechanism to identify the Ca^{2+} channel features of CD20 are still elusive. Meanwhile, rituximab in known to cause Ca^{2+} signaling through CD20 binding, but the Ca^{2+} signaling effects of the two improved monoclonal antibodies, obinutuzumab, and ofatumumab were not reported yet.

Therefore, purpose of this study is demonstration 1) the characterization of CD20 as a SOC Ca^{2+} channel regulated by STIM1 in a Orai1 dependent manner and 2) how the Ca^{2+} signal through SOC mechanism will influence the characteristic or efficacy of each antibody.

Protein interaction between CD20 and STIM1 was increased in store depleted condition, but their interaction was dependent on the presence of orai1. Both rituximab and obinutuzumab showed Ca^{2+} influx from the outside of cells, but CD20 protein interactions with STIM1 had different effects depending on the type of antibody. In the case of rituximab, the effect of CD20 binding to STIM1 was

negligible in the Ca^{2+} influx, whereas the amount of Ca^{2+} influx from the outside were significantly increased in STIM1 co-expression by obinutuzumab. And the ability of obinutuzumab to bind CD20 decreased by siRNA targeting orai1. Subsequently, homotypic adhesion by obinutuzumab didn't occur when the external Ca^{2+} free solution. However, the external Ca^{2+} concentration didn't alter the dose dependent cell death via the direct obinutuzumab binding. Interestingly, external Mg^{2+} concentration altered the rate of the cell death induced by direct obinutuzumab binding.

Therefore, I suggest that the CD20 is a component of ion channel regulated by STIM1 and Orai1. Moreover, the ion channel activity of CD20 could contribute to the B cell depletion efficacy of obinutuzumab via permeating Mg^{2+}.

Key words: CD20, STIM1, SOCE, rituximab, obinutuzumab, ofatumumab, Ca^{2+}, Mg^{2+}

Effect of CD20 Ca^{2+} channel activity on the efficacy of rituximab and obinutuzumab

Woon Heo

Department of Medical Science
The Graduate School, Yonsei University

(Directed by Professor Joo Young Kim)

I. INTRODUCTION

CD20 is a 4 transmembrane protein, one of the MS4A family (MS4A), expressed exclusively in B cells.[1] CD20 is used as the target of antibody for depleting the mature B cell and lymphoma. Those antibodies do not cause total collapse of the adaptive immune response, because pro-B cell and plasma cell do not express CD20 among B cells.[2]

CD20 is known as a raft localized protein which has a raft localizing region in its cytoplasmic C-terminal tail near the fourth transmembrane domain[3]. Especially, rituximab binding to CD20 causes CD20 aggregation into raft region, which is one of the typical characteristics of type1 categorized antibody.[4] Through aggregated CD20, rituximab-like type 1 antibodies enhance the interaction with complement, which in turn causes cell death. In contrast, type 2 antibody, like obinutuzumab, works mainly through the antibody dependent cell mediated cytotoxicity.[5,6] It has been focused on that the Fc region of the antibody determines the action mechanism

of these types of antibodies. But recent reports revealed that antigen recognition modes are also important for the function of antibodies.[7,8] In fact, non-glycosylation form of obinutuzumab, GA101 also showed the similar ADCC activity as glycosylated form of obinutuzumab, in spite of their distinct affinity to the Fc gamma receptor.[5,9] In addition, it is known that the epitope region of rituximab and obinutuzumab are the same extracellular big loop of CD20 according to the epitope finding analysis using amino acid scan. However, the configurations of CD20 bind to antibodies including the binding angles is different according to the structural analysis.[8] Therefore, it seems that the configuration of target protein CD20 and the binding mode of antibodies also contribute to their potency of B cell depletion.

However, the basic molecular mechanism and interactions between CD20 and its antibody was not well understood as much as the clinical efficacy studies of CD20 antibodies. Especially, although previous studies have shown that CD20 transfected cells show SOCE (store operated Ca^{2+} entry) activity greater than mock, indicating that CD20 is a SOC(store operated Ca^{2+} channel) [10,11], there is no molecular mechanism study of the channel activity of CD20 or its effect on antibody function.

Ca^{2+} is not only important to cell growth and death, but also involved in a variety of signaling processes maintain the homeostasis of cells. Intracellular Ca^{2+} is maintained in a few nM level. This Ca^{2+} acts as a signaling material when the concentration is increased by the influx of external Ca^{2+} or efflux from internal Ca^{2+} store. High concentration Ca^{2+} in the cytoplasm that acts as a signal is returned to the low level again by PMCA (plasma membrane Ca^{2+} ATPase), which exports Ca^{2+} to the outside of the cell, or SERCA (sarcoendoplasmic reticulum Ca^{2+} ATPase), which brings Ca^{2+} back into the intracellular Ca^{2+} reservoir. However, in this process, the Ca^{2+} inside the reservoir is gradually consumed, and a mechanism for receiving Ca^{2+} from the outside of the cell is needed. The Ca^{2+} channel which present in the cell membrane activated by the depletion signal of the intracellular Ca^{2+} reservoir is referred to as a ‘store operated Ca^{2+} channel (SOC)’.[12]

STIM1 was first identified as a protein that present increased expression in B-cell lymphocytes and cancer.[13,14] In 2006, it was found as the only regulatory switch

of SOCE.[15,16] STIM1 is a protein with one transmembrane region mainly localized in the ER membrane. The EF hand of STIM1 at the N-terminus detects the Ca^{2+} concentration in the ER and STIM1 controls the opening and closing of the SOC channels such as orai1 in the cell membrane through the C-terminal SOAR (STIM1 orai activating region) region.[17] Since the known all SOC channel such as Orai1, TRPC1, and TRPC4 bind to and being regulated by STIM1, the protein binding to STIM1 has become a decisive criterion for the determining as a SOC channel. As discussed above, CD20 is reported as a SOC channel which is activated by treating Tg (thapsigargin), a drug that depletes Ca^{2+} in the Ca^{2+} reservoir. However, there is no report whether CD20 binds to STIM1. Furthermore, the effect of the other CD20 antibodies on Ca^{2+} signal, except rituximab were not investigated yet. Therefore, understanding the molecular mechanism of Ca^{2+} influx through CD20 and its effects on the efficacy of CD20 antibodies might contribute to not only for the development of antibodies, but also for the prevention from their side effects.

In this study, I investigate the typical characteristics of CD20 as a Ca^{2+} pore which is regulated by store depletion. In addition, The Ca^{2+} influx through CD20 triggered by three different kinds of CD20-antibodies, rituximab, ofatumumab, and obinutuzumab, produced in our lab. Moreover, this Ca^{2+} influx induced by those antibodies have effect on the typical changes of B cells and the efficacy of B cell depleting.

.

II. MATERIALS AND METHODS

1. Cells and transfection

Human B-lymphoma RAMOS cell line was purchased from the Korean Cell Line Bank. Cells were maintained in RPMI1640 media supplemented with 10% FCS and 1% penicillin/streptomycine at 37°C, 5% CO2. HEK 293T cell line was maintained in DMEM media supplemented with 10% FBS and 1% penicillin/streptomycine at 37°C, 5%. For expressing CD20 or STIM1 in HEK cells, Lipofectamin 2000 reagent was used according to the standard protocol recommendations.

2. Reagents and solutions

cell cultures, DMEM culture medium (Dulbecco's modified Eagle medium, 11995-065), RPMI 1640 (Roswell Park Memorial Institute medium, 11875-093), Fetal bovine serum (FBS) (26140-079), Penicillin-streptomycin (15140-122; Gibco, Life technologies™, Carlsbad, CA, USA); Trypsin-EDTA 0.05% solution (25300-062; Gibco, Life technologies™, Carlsbad, CA, USA) were used. For RT-PCR analysis, TRIzol reagent (Invitrogen, Life technologies™, Carlsbad, CA, USA); AccuScript High Fidelity 1st Strand cDNA Synthesis Kit (200436; Agilent Technologies, Santa Clara, CA, USA); Solg™ 2x Taq PCR Smart mix (STD02-M10h; SolGent Co., Daejeon, Korea) were used.

For immunoblotting, NaCl (S7653), Triton X-100 (T8787), Glycerol (G5516; Sigma Aldrich); EDTA (15694, Usb, USB Coporation, Cleveland, OH, USA); Tris Ultrapure (T1501, Duchefa, Haarlem, The Netherlands); Complete proteinase inhibitors (Roche Applied Science, Mannheim, Germany); HCl (084-05425), NaOH (196-05375, Wako, Osaka, Japan); BCA Protein Assay Kit (23227; Pierce™, Thermo Scientific, Rockford, IL, USA); 5x Tricine-SDS sample buffer (KTR020-5), pre-made 4-12% gradient SDS-PAGE gels (KG5012) (KOMA Biotech, Seoul, Korea) were used.

For Ca^{2+} imaging experiments, NaCl (S7653), KCl (P5405), $MgCl_2$ (M8266), Glucose (G6152), HEPES (H3375), $CaCl_2$ (C1016), EGTA (E3889), and Fura-2 AM (F1201; Invitrogen, Molecular probes, Eugene, Oregon, USA) were used.

For immunocytochemistry, 4% Paraformaldehyde (19943), BSA (10857; Affymetrix, Cleveland, Ohio, USA); Horse serum (16050-122, Gibco); Gelatin (G1890), Na_3N (S2002), Phosphate-buffered saline (PBS) (P5493, Sigma Aldrich) were used.

3. Antibodies and fluorescent dyes

Anti-Stim1 (610954; BD Transduction Laboratories™ San Jose, CA, USA), Alexa Fluor-rhodamine (A11004, Invitrogen, Molecular probes, Eugene, Oregon, USA) were used.

4. Generation of Mab-producing CHO cells

To generate cells stably expressing rituximab, obinutuzumab, or ofatumumab, lentiviruses was produced expressing heavy chain or light chain of the three antibodies, GNT3, or MAN2A (for the design of the lentiviruses, see Suppl Fig 1). CHO-RTX and CHO-OFA cells were generated by co-transduction of CHO-K1 cells (ATCC) with the same titers of HC and LC viruses followed by double selection with growth medium containing 10 μg/mL puromycin (Sigma) and 10 μg/mL blasticidin S (Sigma) for a week. CHO-K1 cell was transduced with LVX-GNT-Hygro and LVX-MAN2A-Bleo viruses and selected with 500 μg/mL of hygromycin (AG Scientific) and 100 μg/mL of zeocin (Invitrogen) for a week. The resulting CHO-GE cell was transduced with lentiviruses expressing HC and LC of obinutuzumab and selected with 10 μg/mL puromycin and 10 μg/mL blasticidin S. Over-expression of myc-rGnT3 was proved by WB analysis with anti-myc antibody and mRNA expression of rGnT3 and Man3 was proved via RT-PCR analysis.

5. Production and purification of Mab

CHO-RTX, CHO-GE-OBI, and CHO-OFA cells grown to 80% confluency in RPMI containing 10% FBS and 10 μg/mL ciprofloxacin (Sigma) were washed twice with PBS and refreshed with EX-CELL® CD CHO Serum-Free media (Sigma) containing 1 mM sodium butyrate. Conditioned media containing Mab were obtained by further incubation for 10 days at 30°C in 5% CO2/95% air. Antibodies were purified via affinity chromatography using protein A-Sepharose bead (GE Healthcare Life Sciences). Buffer-changed and concentration was conducted by ultrafiltration with Amicon® Ultra-2 before filter-sterilization and storage. The proteinous characteristic of antibodies were analyzed by SDS-PAGE and coomassie blue staining and quantification of each antibody concentration was indirectly measured via substraction according to relative band intensity of 0.2, 0.4, 0.8, 1.6, 3.2 ug of BSA as standard.

To produce the rituximab, obinutuzumab, and ofatumumab in CHO cells, DNA sequence of each mAb were delivered from Drugbank(rituximab), patent document (Sequence 3 from patent US 6897044- heavy chain, Sequence 1 from patent US 6897044- light chain) and then each light and heavy chain DNA poly nucleotide sequence was synthesized from Bioneer company then inserted into pLenti6 viral vector. Each light and heavy chain was transfected into HEK cells to produce Lentivirus particle. Then both light and heavy chain expressing Lentivirus was infected in CHO cells then infected cells were selected with blasticidin and Puromycin. The selected cells were multiplied to 5 flasks of T75 then sodium butyrate was treated to erase any methylated DNA to increase the expression level of antibody. The cell media grown for 10 days was collected then secreted antibody was collected using protein A beads. The concentration of antibody was measured with SDS-PAGE and coomassie staining with BSA as a standard. Since obinutuzumab is glycol-engineered antibody having highly Gln residue in Fc region, the glyco-CHO cells was produced which is rGnT3 and MAN2 over-expressing cells via the selection through resistant from hygromycin and zeocin after infection of LVX-GNT-Hygro and LVX-MAN2A-Bleo viruses. Both expression was checked with myc-rGnT3 protein and

mRNA of each construct.

6. Reverse-transcriptase PCR analysis

Total RNA was extracted with TRIzol reagent according to the manufacturer's instructions. cDNA was synthesized using AccuScript High Fidelity 1st Strand cDNA Synthesis Kit according to the manufacturer's instructions. RT-PCR was performed in triplicate using Solg™ 2x Taq PCR Smart mix. Each RT-PCR reaction contained 100 ng of cDNA. The thermocycling conditions of RT-PCR were an initial denaturation at 95 °C for 5 min followed by 31~37 cycles of 95°C for 30 sec, 58°C for 40 sec and 72°C for 40 sec, and a last extension at 72°C for 7 min.

The primer sets are provided as follows (S, sense; AS, antisense) were used for PCR analyses for CD20, S, 5'- TCTTCACTGGTGGGCCCCAC-3' and AS, 5'-CCTCTTTGCTGCCATTTCTGGAAT-3'; for Stim1, S, 5'-GGAAGACCTCAA TTACCATGAC-3' and AS, 5'-GCTCCTTAGAGTAACGGTTCTG-3'; for Orai1, S, 5'-TGTTTGCCCTCATGATCAGCAC-3' and AS, 5'-AAACTCGGCCAGCTCATT GAG-3'.

7. Immunoblotting

HEK293T cells were seeded into 6-well plates at 1 x 10^6 cells/well and incubated at 37 °C in an incubator enriched with 5% CO_2 atmosphere incubator overnight. Then, cells were lysed in lysis buffer [150 mM NaCl, 5 mM Na-EDTA, 10% glycerol, 20 mM Tris-HCl pH 8.0, 0.5% Triton X-100, and complete proteinase inhibitors]. Protein concentration was quantified using a colorimetric method Bradford Protein Assay according to the manufacturer's instructions. The lysates (40 μg of protein) were eluted with 5x Tricine-SDS sample buffer, and the eluted lysates were separated on pre-made 4-12% gradient SDS-PAGE gels. Primary antibodies included anti-flag, anti-myc, and caveolin; appropriate secondary antibodies were used.

8. Single live cell $[Ca^{2+}]_i$ imaging

Single live cell $[Ca^{2+}]_i$ imaging was measured by recording $[Ca^{2+}]_i$ with Fura-2

AM labeling at dual excitation wavelengths of 340/380 nm ratiometrically. 5-10 x 10^4 HEK293T cells were plated in 18 mm φ cover glass (Paul Marienfeld GmbH & Co. KG, Lauda-Königshofen, Germany). After appropriate transfection, the cells were added with cell-permeable 2 μM Fura-2 AM and incubated at 37 °C in an incubator enriched with 5% CO_2 atmosphere incubator for 30 min, and trapped Fura-2 fluorescence was measured with a spectrofluorometer (Photon Technology International, Birmingham, NJ, USA). Cells were perfused with a solution containing 150 mM NaCl, 5 mM KCl, 1 mM $MgCl_2$, 10 mM glucose, 10 mM HEPES (pH 7.4 adjusted with NaOH) containing either 1–2 mM $CaCl_2$ or 5 mM EGTA (to chelate any Ca^{2+} in the solution). The osmolality of all solutions was adjusted to 310 osm with the major salt. The Fura-2 ratio was recorded using dual-excitation wavelengths at 340 and 380 nm, and emission wavelengths above 510 nm were monitored. Cells were treated with 5 μM TG which inhibits the sarcoendoplasmic reticulum Ca^{2+}-ATPase. Cells were treated with 2mM $CaCl_2$ and then each single whole cell boundary was drawn and analyzed the intracellular Ca^{2+} concentrations $[Ca^{2+}]_i$) during the experiments.

9. Immunocytochemistry

HEK cells were transfected with pcDNA3.1-mCherry CD20 plasmid then the CD20 specific recognition of each purified antibody were tested with immunocytochemistry. HEK cells cultured in 18 mm cover slips and pcDNA3.1-mCherry-CD20 plasmid were transfected with Lipofectamine2000 (Invitrogen, cat no. 11668019). After 48 hours, cells were fixed with 3.7% formaldehyde in PBS, then non-specific binding were blocked by 30 min incubation in blocking solution (5% horse serum, 1% gelatin, 5% BSA in PBS). rituximab, ofatumumab, and obinutuzumab were treated for 1 hour then 2nd anti-Fc specific human IgG conjugated with FITC was treated to bind each 1st antibodies. DAPI (5ug/ml) was used for nucleus staining. CD20 expressing cells were identified via the fluorescence of tagged mCherry (red) and the binding of each antibody was visualized by FITC fluorescence of 2nd antibody. Image was taken from the Zeiss 780 confocal

microscopy.

In RAMOS cells, each antibody was treated at 37C for 15 min in presence of absence of Ca^{2+} in PBS then fixed with 3.7% formaldehyde for 5 min at RT then washed with PBS for three times. 2nd anti-Fc specific human IgG conjugated with FITC was treated to bind each 1st antibodies. To permeabilize the cell membrane, 0.1 % triton in PBS was treated then goat anti-CD20 (Santa-cruz, cat no. sc-7735) were treated then anti-goat IgG specific 2nd antibody conjugated with Alexa568 were used to visualized the total CD20. Caveolin were stained with anti-caveolin1 antibody (enogene, cat no. E18-6386) then it was visualized with anti-rabbit IgG specific 2nd antibody conjugated with Alexa 350 (blue).

10. Measurement of complement cell death, antibody mediated cell death, and direct antibody mediated cell death

For measure various cell death assay, 5 x 104 cells/well RAMOS cells were plated in 12 well plate then 1uM calcein-AM was treated for 30 min in 37C for staining of healthy viable cells. Cells were resuspended into 500ul of media then indicated dose of antibody (0.1, 0.3, 1. 3, and 10ug/ml) were treated for 10 min. Next step is diverged into CDC, ADCC, and direct antibody binding mediated cell death via used materials. For measurement of complement dependent cell death assay, rabbit complement MA were added a quarter of the total volume and incubated in 37C CO2 incubator for 2 hr. For antibody-dependent cell mediated cell death, same method with complement dependent cell death assay was used. After each concentration of antibodies treatment, purified PBMC (PBMC: RAMOS = 5:1) was incubated at 37C CO2 incubator for 4 hr. For measurement of direct antibody binding mediated cell death, cell treated with indicated antibodies were incubated at 37C incubator for 24 hr without any complement or effector cells. % of cell lysis (% of fluorescence loosing cells number among 10,000 counted total cell) was calculated by FACSVerse (BD Biosciences) and FlowJo software.

11. Purification of PBMC cells

PBMC was purified with the total blood from health donors who was voluntarily participated in our experiment according to IRB procedure approved by the committee of Yonsei severance IRB board. All procedures were approved by IRB (#4-2016-0600). Briefly, 4 ml of blood sample were centrifuged with 1600 x g. Cell removed serum were resuspended with 8 ml of PBS and loaded onto 4 ml of ficoll (HISTOPAQUE-1077, Sigma, 10771) then centrifuged at 400 g for 35 min at 20℃ to separate white blood cells from red blood cells. The white blood cell layer was collected into new tubes then washed three times (centrifuge 300g for 10 min) with RPMI media to completely remove the platelet. Purified PBMC cells was counted then incubate in RPMI media until use.

12. Measurement of Ca^{2+} influx by antibodies via FACS

Ca^{2+} influx through CD20 was measured using Ca^{2+} sensitive fluorescence dye Fluo-4 and FACS. To variate the expression level of CD20, HEK cells were transfected with 0.4 ug and 4 ug of pcDNA3.1-CD20 using Lipofectamine2000 for 48 hours to produce high and low CD20 expressed HEK cells respectively. Celle were detached from the plate with the sheered flow of media to keep the integrity of surface expressed CD20, then cells were incubated with 2 uM Fluo-4 for 30 min. Then cells were resuspended with 2 mM Ca^{2+} Regular solution (mM: 140 NaCl, 5 KCl, 1 MgCl2, 2 CaCl2, 10 glucose and 10 HEPES (pH 7.4 adjusted with NaOH, 310 osmolality with NaCl). 1X 105 cells were used for fluorescence counting and no Fluo-4 treated cells were used for negative control of fluorescence. Before treat antibody, basal status of $[Ca^{2+}]_i$ was measured by fluorescence level of Fluo-4 loaded cell. Then the change of $[Ca^{2+}]_i$ by rituximab, ofatumumab, and obinutuzumab including Human IgG (control) were measured after 10 min after treatment and cross linking antibody (goat anti-Human IgG Fc specific) was also used at the end of the measuring to confirm the capability of cells to produce Ca^{2+} influx. Same method was used to RAMOS cells and $5x10^5$ cells were used and $5x10^4$ cells were counted.

13. Quantification of Raft localized CD20 through Triton solubility test

Aliquots of 5×10^6 RAMOS cells per sample were incubated at 37°C for 30 min in complete culture medium either alone or supplemented with 10 μg/mL antibody or 10 μg/mL isotype control. After centrifugation at 500g for 10 min,

14. Statistical analysis

Data are presented as the means ± standard error of the mean. Statistical analysis was performed with Student's t-test or with analysis of variance (ANOVA), followed by Tukey's multiple comparison and one-way or two-way ANOVA tests using the GraphPad Prism software package (version 5.0), as appropriate. $P<0.05$ was considered statistically significant.

III. RESULTS

1. Ca^{2+} entry via CD20 in CD20 overexpressing HEK Cells

HEK cells expressing either exogenous CD20 or STIM1 were loaded with fura-2 AM, the Ca^{2+}-sensitive dye, and the fluorescence changes in each single cells were recorded. Intracellular Ca^{2+} stores were depleted by Tg(Thapsigargin). The Ca^{2+} influx activity of CD20 was compared with Orai1 using HEK cells co-expressing Orai1 and STIM1 as positive control. To confirm the Ca^{2+} influx activities of CD20 and Orai1 enhanced by STIM1 interaction, STIM1$^{\Delta ERM}$ was used as a negative control which does not have the channel binding domain. TG treatment in the absence of extracellular Ca^{2+} cause the depleting the Ca^{2+} in ER (endoplasmic reticulum) and increase $[Ca^{2+}]_i$. After reaching the basal level of $[Ca^{2+}]_i$, the subsequent perfusion of 2 mM Ca^{2+} solution induced a large increase of $[Ca^{2+}]_i$ in CD20 overexpressed cells (Fig. 1A). Basal $[Ca^{2+}]_i$ level of each condition were quantified from the resting level of ratio (Fig. 1C) and the relative Ca^{2+} influx activities were summarized by the largest ratio value after 2 mM Ca^{2+} perfusion (Fig. 1D). There was no big difference in basal $[Ca^{2+}]_i$ level among groups. However, the relative Ca^{2+} influx activity was increased in CD20 transfected cells. Although not greater than that of the positive control, relative Ca^{2+} influx activity was further increased in the group co-expressing CD20 and STIM1 and this increase disappeared when co-expressed with STIM1$^{\Delta ERM}$. Taken together, CD20 has the potential to interact with and regulated by STIM1 as SOC channel.

2. Increased protein interaction of CD20 and STIM1 in Ca^{2+} store depleted condition and identification of interaction region

Previously, CD20 is known to as a Ca^{2+} channel and Ca^{2+} imaging data indicated that the Ca^{2+} influx is regulated by SOC mechanism. To check whether CD20 interact with STIM1 as a SOC channel, co-IP (immuno-precipitation) and immuno-cytochemistry assayed for CD20 and STIM1 interaction. As a result, CD20 and STIM

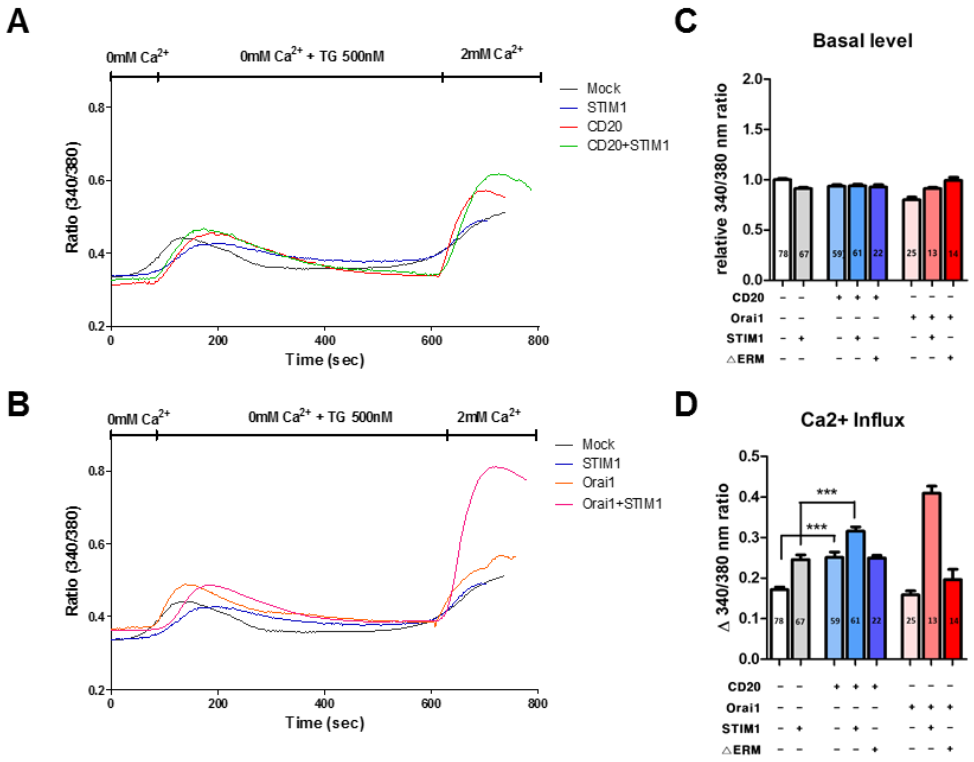

Figure 1. CD20 is a store operated channel regulated by STIM1. (A) Representative trace of $[Ca^{2+}]c$ changes by CD20 depending on STIM1 interactions in HEK cells. CD20 was co-expressed with pcDNA3.1(Mock), STIM1, and $STIM1^{\Delta ERM}$ in HEK cells then the live imaging of Fura-2 AM loaded each single cell was recorded. (B) Representative trace of $[Ca^{2+}]c$ changes by Orai1 depending on STIM1 to compare the magnitude of Ca^{2+} influx mediated by CD20 and STIM1. (C) The level of basal $[Ca^{2+}]c$ in the each indicated condition. The begging ratio were used for the quantification and the fold of pcDNA3.1 transfected cells mock cells level were presented as a graph. (D) The relative Ca^{2+} influx activities. The traces of indicated number of cells were used for analysis. *p<0.05, **p<0.01, ***p<0.001, and ns, not significant.

were found to interact with each other, and their association was further enhanced by Tg induced store depletion (Fig. 2A). Moreover, $STIM1^{D76A}$, the constitutively active mutant of STIM1 showed the strongest interaction with CD20 in unstimulated condition.

Next, to determine the binding region for CD20-STIM1 interaction, C-terminal truncated CD20, $CD20^{\Delta CT}$ was used for co-IP with STIM1. Since the truncated $CD20^{\Delta CT}$ failed to interact with $STIM1^{D76A}$, the C-terminus region of CD20 is supposed to be essential for their interaction (Fig. 2B-C). Their increased interaction in store depletion was also observed in immunostaining analysis. HEK293 cells co-transfected CD20 and STIM1 treated with Tg (Fig. 2D). Their co-localization in puncta at Tg treatment indicate that the store depletion cause CD20 and STIM1 interaction in HEK cells.

3. Ca^{2+} influx via CD20 regulated by STIM1 is dependent on Orai1

To further explore the mechanism underlying the Ca^{2+} influx by CD20, whether CD20 channel activity is dependent on the existence of Orai1 was investigated. The small interference RNA targeting Orai (siOrai1) inhibited relative Ca^{2+} influx activities of either CD20 or STIM1 expressed cells even in samples that are expressed together (Fig. 3A). And at a gradual increase in Orai1 expression, the amount of CD20 interacting with STIM1 also increased (Fig. 3B). These results indicate that CD20 constitute the channel complex with Orai1 and Ca^{2+} influx via CD20 regulated by STIM1 is dependent on orai1. These data imply that the store operated property of CD20 is probably dependent on the Orai1 regulation by STIM1, rather than the direct regulation by STIM1.

4. Expression of CD20, STIM1 and Orai1 and their interaction in RAMOS cell

Next, the channel components expression was confirmed mRNA and protein level. Then, to investigate to their physiological interaction, co-IP experiments was performed using the lysate form RAMOS cell, a human Burkitt's lymphoma cell

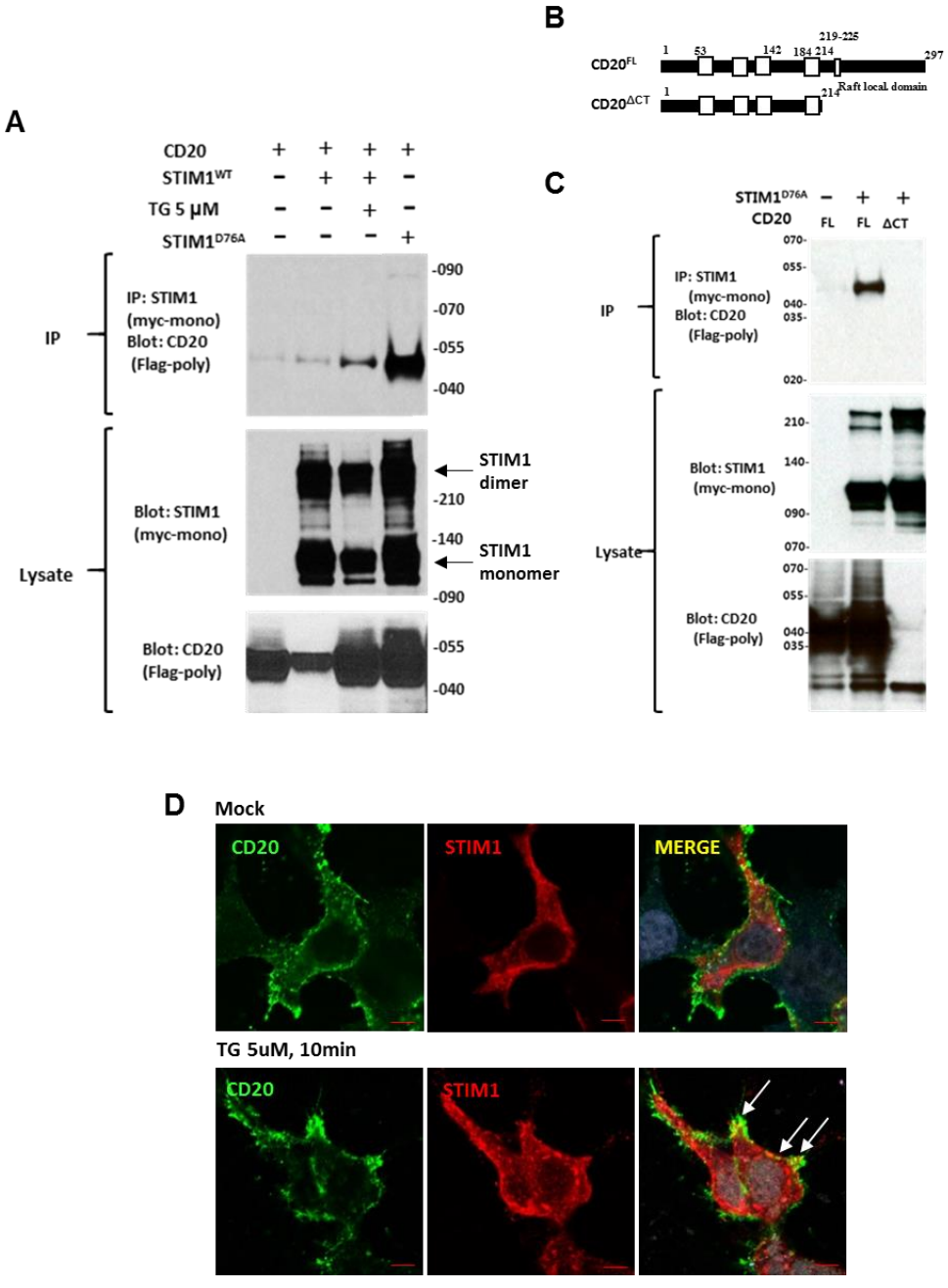

Figure 2. Enhanced protein interaction of CD20 and STIM1 in Ca^{2+} store depleted condition. (A) Store depletion enhances protein interaction of CD20 and STIM1. Immunoprecipitated STIM1 protein was observed to show the CD20 and STIM1 protein interaction in HEK cells over-expression with flag-CD20 and myc-STIM1. 5 uM Tg and STIM1D76A (constitutive active form) were used to show the enhanced protein interaction between CD20 and STIM1 in store depletion condition. Expressed amount of CD20 and STIM1 were compared using WB analysis with monoclonal anti-myc antibody for STIM1 and polyclonal anti-flag antibody for CD20. (B) The scheme of CD20 protein structure about full length CD20 and C-terminal truncated $CD20^{\Delta CT}$ (C) Interaction of CD20 with STIM1 in mediated by internal C-terminal region of CD20. Immunoprecipitation assay show that the internal C-terminal truncated $CD20^{\Delta CT}$ failed to interact with $STIM1^{D76A}$. (D) CD20 and STIM1 localization in normal condition (upper) and store depleted condition (5 uM Tg for 10 min) (bottom) in HEK cells. CD20 and STIM1 were labeled with mouse anti-Flag (2nd antibody conjugated with FITC (green)) and anti-STIM1 (2nd antibody conjugated with rhodamine (red)), respectively. DAPI (blue) was used for nucleus staining. Merged images showed their co localization (yellow) upon store depletion condition. White arrows indicate the co-localized CD20 with STIM1. Bar indicated 5um.

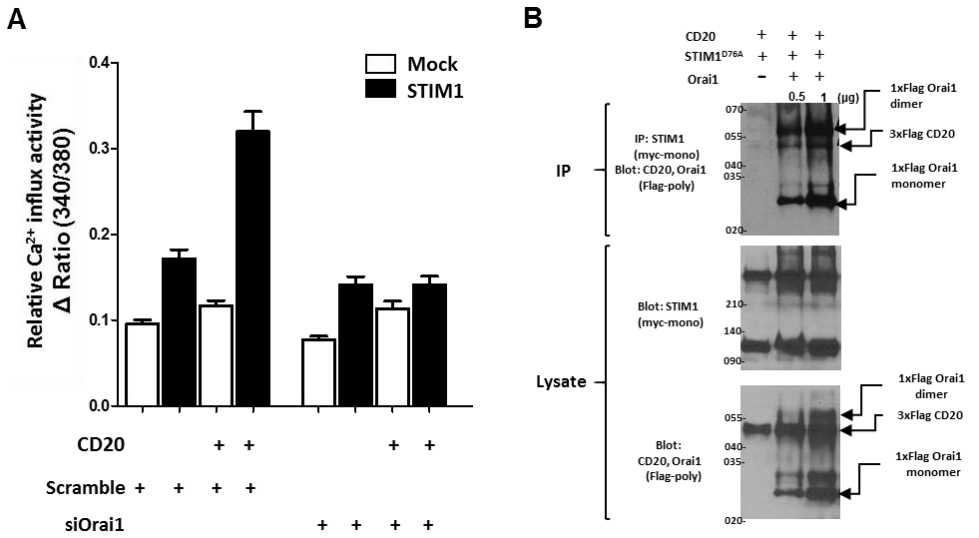

Figure 3. Ca^{2+} influx via CD20 regulated by STIM1 is dependent on Orai1. (A) Orai1 dependent STIM1 regulation of Ca^{2+} influx activity through CD20. siRNA for Orai1 was used to determine whether CD20 regulation by STIM1 is dependent on Orai1. The relative Ca^{2+} influx activity was quantified Orai1 dependent protein interaction of CD20 and STIM1 in HEK cells using Fura-2 AM fluorescence recording. Relative activity was summarized as folds of scramble only treated cells. (B) Enhanced protein interaction of CD20 and STIM1 upon increased expression of Orai1. Immunoprecipitation assay using monoclonal anti-myc antibody for myc-$STIM1^{D76A}$ was performed after 0.5 and 1 ug flag-Orai1 with 3xflag-CD20 overexpression. Each protein expression was confirmed by western blot using anti-myc and anti-Flag antibodies with lysates and precipitated Flag-Orai1 and 3xflag-CD20 proteins via by monoclonal anti-myc antibody were detected with polyclonal anti-flag antibody. Each protein was indicated as shown in pictures.

line known to express CD20. In RT-PCR analysis, endogenous STIM1 and orai1 mRNA expression of RAMOS cells was observed with CD20 (Fig. 4A). In addition, WB analysis for endogenous protein expressions showed that all three proteins were expressed in RAMOS cells. STIM1 is observed as monomer and dimer and orai1 protein also exhibit its monomeric, dimeric and trimeric configurations. (Fig. 4B-C). In RAMOS cells, CD20 dominantly exist as a monomer in WB analysis. However, CD20 monomers failed to interact, but dimer and tetramer of CD20 interacted with STIM1 (Fig. 4D). This interaction was further strengthened by Tg, which corresponds to the previous IP experimental data using HEK cells heterologous expression system.

5. Successful purification of rituximab, obinutuzumab and ofatumumab and their quantification

To produce the antibodies required for the experiment, lentivirus system was used the for LC (light chains) and HC (heavy chains) expression. In the case of LC, the variable region and the constant region were totally synthesized, while in the case of HC, the variable region was synthesized and connected with the constant region delivered from the IgG sequences of health volunteer donating blood (Fig. 5A). To make obinutuzumab, a glycosylation-engineered antibody on the Fc region, two kinds of necessary enzymes were cloned (Fig. 5B) then confirmed their mRNA (Fig. 5C) and protein expression of rGNT3 (Fig. 5D) in CHO-K1 cells (Fig. 5B). The antibody presence and amount were checked during each step of purification and the size of LC (~20 kDa) and HC (~55 kDa) were also confirmed at the reducing condition of SDS-PAGE (Fig 5E). To quantify the amount of antibodies, all three antibodies were separated in SDS-PAGE of non-reducing condition and visualized with coomassie blue staining (Fig. 5F). Indicated amount of BSA were used for the standards for protein quantity. These all data demonstrated that the successful establishment for the production of rituximab and ofatumumab antibody including the glycol-engineered obinutuzumab.

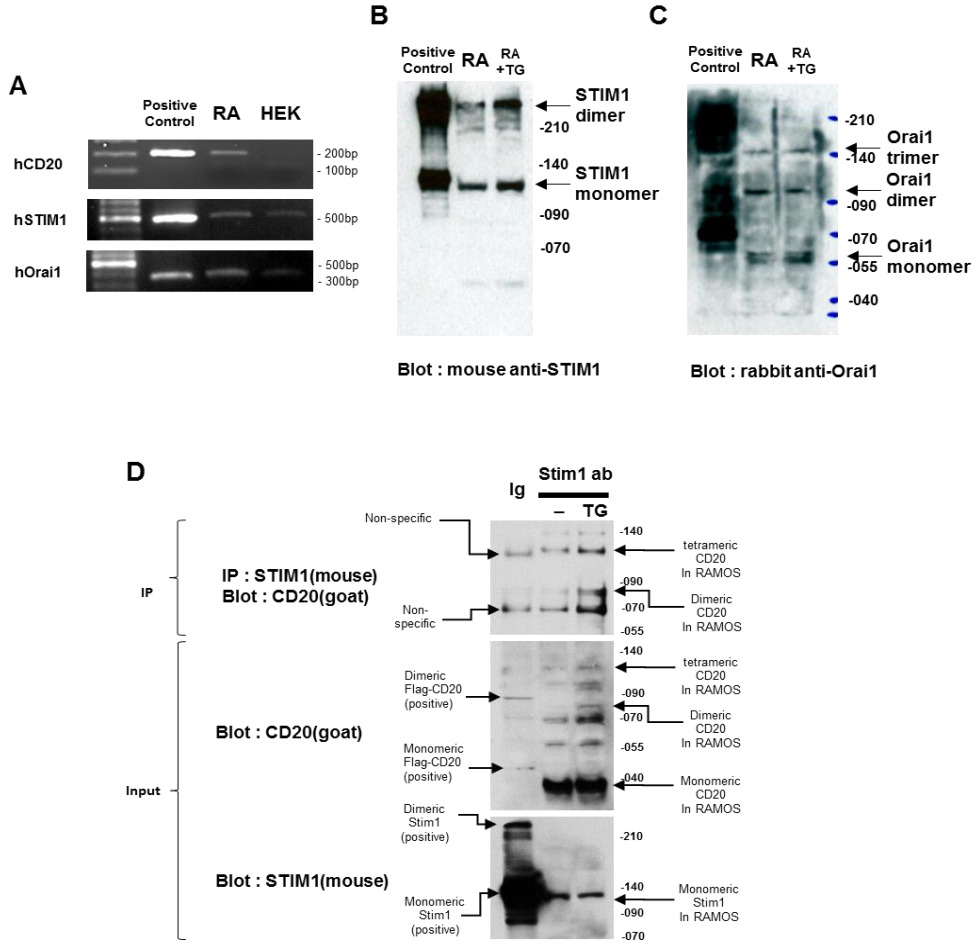

Figure 4. Expression of CD20, STIM1 and Orai1 and their interaction in RAMOS cell. (A) mRNA expression of CD20, Orai1 and STIM1 was observed via RT-PCR analysis with RAMOS cells. Total mRNA was purified from RAMOS cells and HEK cells then cDNA was synthesized. Each clone for over-expression was used for positive control. PCR products 290bp, 484bp, and 358bp were indicated the expression of CD20, STIM1, and Orai1 in RAMOS cells. Protein expressions of CD20 (B), STIM1 (C) and Orai1 (D) were checked in RAMOS cell lysate in normal and store depletion condition with 5 uM Tg. Goat anti-CD20 antibody, mouse anti-STIM1 antibody, and rabbit anti-Orai1 antibody were used. Each configuration of proteins was indicated as shown. Clone over-expressed lysate was used for positive

control for WB. (E) Endogenous protein interaction of CD20 and STIM1 was observed in immunoprecipitation assay using RAMOS cell lysate. Resting and store depleted condition lysate was immunoprecipitated with monoclonal anti-STIM1 antibody and precipitated CD20 were identified with goat anti-CD20 antibody. Mouse IgG were used for experiment control for IP analysis. In inputs, each over-expressed CD20 and STIM1 was used for the positive control for WB. Each protein was indicated as shown in picture.

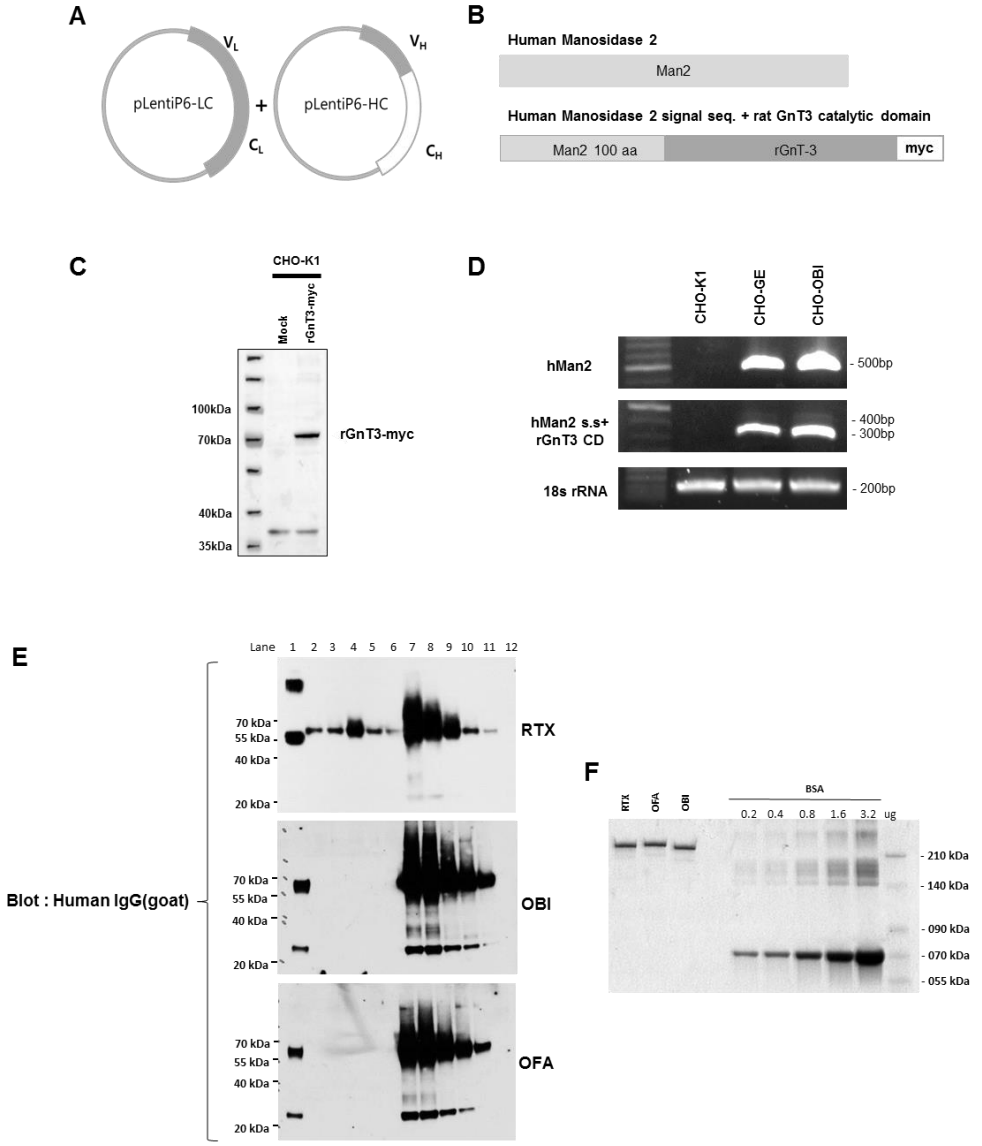

Figure 5. Successful purification of rituximab, obinutuzumab and ofatumumab and their quantification. (A) Schemes for light and heavy chain of monoclonal antibody expression in lentivirus production. Poly-nucleotide synthetized regions were indicated by gray region and RT-PCR delivered region from IgG were indicated by white region. (B) Schemes for glycosylation engineering enzyme used for

establishing the glycol-engineered CHO-K1 cells. Human Mannosidase 2 and rat GnT-3 enzyme fused with signal sequence from human Mannosidase 2 (100 amino acids) were used. rGNT3 with mannosidase signal sequence were tagged with myc for protein expression detection. (C) Expression of rGNT3-myc in glycol-engineered CHO-K1 cells was identified with anti-myc antibody. (D) mRNA expression of human Man2 and rGNT3 with hMan2 signal sequence was confirmed by RT-PCR analysis. 330 bp hMan2 and 318 bp rGNT3 were indicated that the glycol-engineered CHO-K1 cells and obinutuzumab producing glycol-engineered CHO-K1 cells successively expressed both enzymes. 18s rRNA were used for comparison of mRNA used. (E) The purification procedure of rituximab, obinutuzumab, and ofatumumab were shown by the presence of each monoclonal antibodies in purification steps. Lane1, 50 ug of rituximab; lane 2, pre-binding of media; lane 3, post binding of media; lane 4, first washing; lane 5, 2nd washing; lane 6, 3rd washing; lane7, 1st elution; lane 8, 2nd elution; lane 9, 3rd elution; lane 10, 4th elution; lane 11, 5th elution; lane 12, 1% triton X-100. (F) Quantification of monoclonal antibodies using BSA protein standards. 0.2, 0.4, 0.8, 1.6 and 3.2 ug of BSA and 2 ul of final dialysis monoclonal antibodies were SDA-PAGEed in non-reducing condition then coomassie staining was performed to visualize proteins. Completed configuration of antibodies was identified in 280 kDa. Intensity of protein band were quantified by Multiguige software.

6. Validation of accuracy of three antibodies through the binding specificity test, acknowledged B cells changes upon their binding, and the efficacy of three antibodies on B cell depletion.

I firstly confirmed their binding specificities by immunostaining assay using mCherry-CD20 expressed HEK cells. Immunostaining with each antibody revealed that only mCherry-CD20 expressed on the cell membrane was recognized by three antibodies (Fig. 6A). To confirm that the effects of antibodies binding were matched with previously reports, the capping of CD20, a typical characteristic of type 1 antibody, and the homotypic adhesion of cells, a typical characteristics of type 2 antibody were observed after the treatment of three antibodies in RAMOS cells. As same as previous reports, rituximab and ofatumumab, but not obinutuzumab caused the capping of CD20. In case of the homotypic cell adhesion, obinutuzumab, but not rituximab and ofatumumab caused the aggregation of RAMOS cells as similar to previous reports. Next, to test their immune function as mAbs, antibody mediated direct cell death(DCD), complement dependent cell death (CDC), and effector cell mediated cell death (ADCC) were conducted with RAMOS cell (Fig. 6D-F). As already reported, type 1 antibody obinutuzumab only showed DCD and this effect show dose-dependent manner. On the other hand, under CDC condition, rituximab and ofatumumab showed up to 100% cell lysis ability for 2 hr incubation whereas obinutuzumab, only showed the half of activity. In ADCC analysis, the cell lysis was almost not occurred by rituximab and ofatumumab, but obinutuzumab showed significant (20%) cell death treated with 10 ug/ml antibody with effector cell (RAMOS : PBMC = 1 : 5). These data demonstrated that rituximab, obinutuzumab, and ofatumumab was successively produced having the acknowledged function of mAb.

7. Binding of three antibodies trigger Ca^{2+} influx from the extracellular space

Prior to investigating the effect of channel property of CD20 on antibody

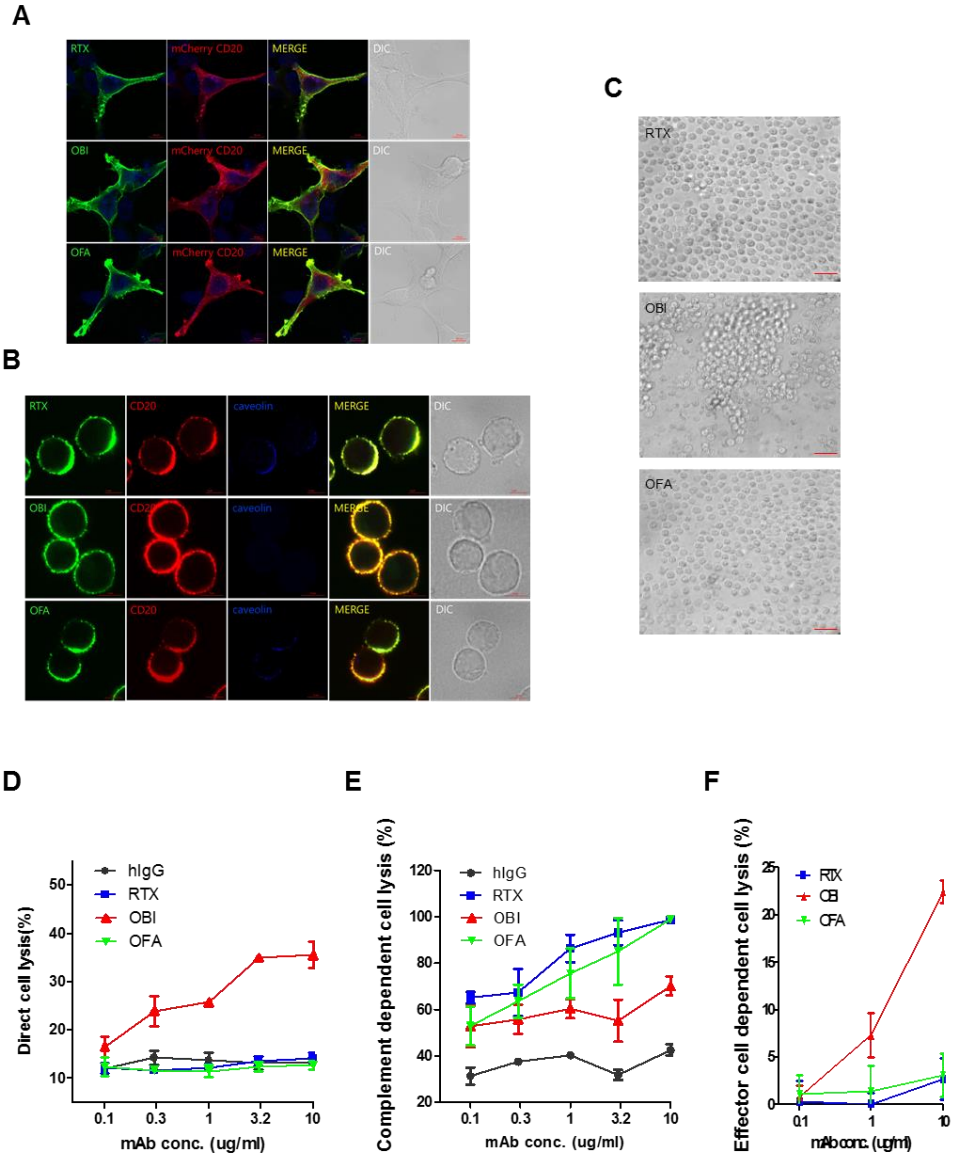

Figure 6. STIM1 controls Orai1 localization in the cell periphery. (A) Binding accuracies of rituximab, obinutuzumab, and ofatumumab were confirmed by immune staining with mCherry-CD20 expressed HEK cell. Among cells, only mCherry-CD20 expressed cells showed each antibody bindings via FITC conjugated anti-human Ig Fc specific secondary antibody. Nucleus was stained with DAPI. DIC images wand DAPI staining showed how many cells were presented in each images. Bar indicates

5um. (B) RAMOS cell treated with each antibody were fixed then the localization of each antibody according to CD20 movement were observed to confirmed that the produced antibodies cause the representative phenomenon in RAMOS cells. To visualize caveolin, anti-caveolin1 antibody was used with Alexa350-conjugated 2nd antibody. To confirmed the CD20 localization in each monoclonal antibody localization, goat-anti-CD20 antibody was used with rhodamine conjugated anti-goat 2nd antibody. Bar indicates 5uM. DIC images shows the overall morphology of RAMOS cells. (C) Homotypic cell adhesion induced by rituximab, obinutuzumab, and ofatumumab were observed after 15 minutes of antibody treatment in 37℃. Only obinutuzumab showed the aggregation of cells as previously known. Bar indicates 25 um. Direct antibody binding mediated cell death (D), complement mediated cell death (E) and effector cell mediated cell death (F) were tested to confirmed with dose dependent increase efficacies of antibodies (0.1, 0.3, 1, 3.2 and 10 ug/ml). Human IgG was used for control.

function, whether Ca^{2+} enters the cell when the antibody binds to CD20 must be observed. To demonstrate this, alteration of intracellular Ca^{2+} concentrations treated by three antibodies were measured according to time under different external Ca^{2+} conditions. When external Ca^{2+} was 2 mM, intracellular Ca^{2+} concentration increased with antibody binding to CD20 in both rituximab and obinutuzumab (Fig. 7A). This is an antibody-specific response compared to no fluorescence change in the control antibody. On the other hand, when external Ca^{2+} was adjusted to 0 mM, no increase in fluorescence was observed (Fig. 7B). This data suggested that the binding of rituximab and obinutuzumab cause the Ca^{2+} influx from outside of cells through CD20.

8. Channel activity of CD20 is enhanced by localization to the non-raft region as a result of forming channel complex with STIM1

To test whether the Ca^{2+} influx induced by rituximab or obinutuzumab is changed by STIM1 expression, the Ca^{2+} influx was measured with GCamp-CD20 fluorescence changes in mock or STIM1 over-expressed HEK cells with FACS analysis. While rituximab didn't make any variation, obinutuzumab treatment induced relative Ca^{2+} influx activity to almost double in STIM1 co-expressed cells than only GCamp-CD20 expressed cells (Fig. 8A). And the amount of obinutuzumab binding was also decreased in STIM1 siRNA treated cells. (Fig. 8C).

Previous studies have shown that rituximab induce moving of CD20 to lipid raft. Because this lipid raft area is resistant to triton, the antibody bound to raft localized CD20 remains in cells after washing with 0.5% triton. On the other hand, the antibodies are washed away after obinutuzumab binding, which indicated that the obinutuzumab bound CD20 is localized in non-raft region in cells (Fig. 8D). STIM1 siRNA treated RAMOS cells showed that the triton resistant portion of obinutuzumab bound CD20 was increased and the washable portion of obinutuzumab bound CD20 was decreased (Fig. 8E).

Accordingly, I suggest that CD20 interact with STIM1 has high affinity to bind obinutuzumab and seems to localize in the non-raft region, which might contribute

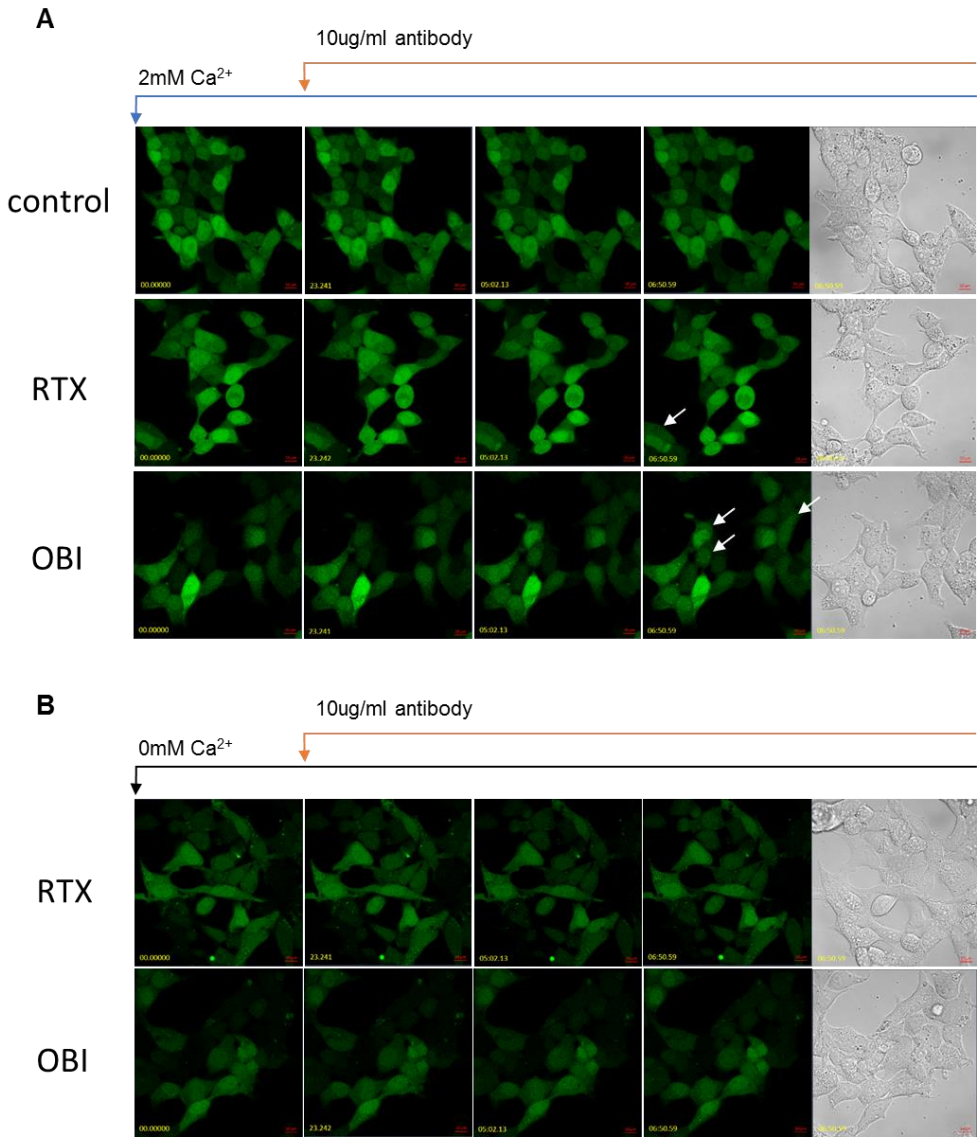

Figure 7. Binding of three antibodies trigger Ca^{2+} influx from the extracellular space (A) Treatment of 10 ug/ml anti-goat CD20 (C-term) as control, rituximab, obinutuzumab in HEK cells expressing CD20 cause the Ca^{2+} influx from the external space. HEK cell expressing CD20 were stained with Fluo-4-AM then Ca^{2+} changes upon rituximab were monitored confocal microscopy for the time dependent changes

of intracellular Ca^{2+} changes. Arrow indicate the changed Fluo-4 fluorescence upon rituximab treatment. Bar indicates 5um and yellow number indicate the time at pictured. (B) Same experiment but used Ca^{2+} free external solution was performed the changes the intracellular Ca^{2+} caused by Ca^{2+} influx from the outside of cells.

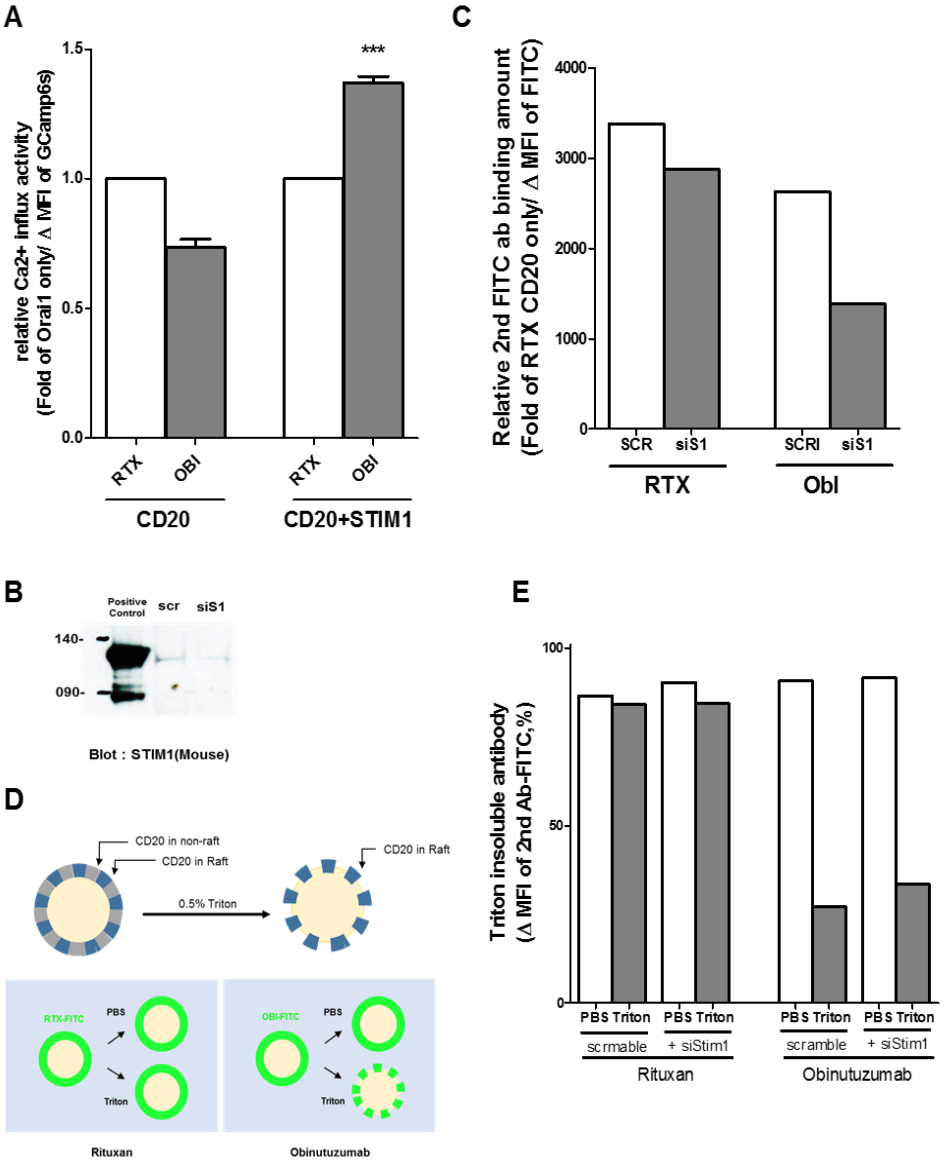

Figure 8. Channel activity of CD20 is enhanced by localization to the non-raft region as a result of forming channel complex with STIM1. (A) rituximab and obinutuzumab induced Ca^{2+} influx activity was measured by fluorescence changes of GCamp 6.S-CD20. To test the effect of STIM1 binding to CD20, mock or STIM1

was co-expressed with GCamp6.S-CD20 in HEK cell. The fluorescence changes after antibody treatment with 2 mM Ca^{2+} were measured with FACS, then the increased fluorescence was summarized as a fold of CD20 only expressed HEK cells treated with rituximab. ***p<0.001. (B) Protein expression of STIM1 significantly reduced by siRNA in RAMOS cells. (C) To test binding property of CD20 upon STIM1 knockdown, RAMOS cells transfected with scramble or siSTIM1 were treated with rituximab or obinutuzumab, then their binding amount were quantified by the FITC conjugated secondary antibodies. In siSTIM1 treated condition, the antibody CD20 were decreased. (D) Cartoon for the quantification of raft localized CD20 using triton X-100 solubility test. Raft localized CD20 and non-raft localized CD20 were indicated with blue and gray color, respectively. Treatment of 0.5% triton X-100 treatment solubilized the non-raft localized CD20 (gray), then raft localized CD20 were left. Since rituximab binds to the raft localized CD20 and obinutuzumab binds to non-raft localized CD20. 0.5% triton treatment caused no fluorescence changes in FITC-rituximab bound CD20, but it caused large decreased fluorescence FITC-obinutuzumab bound CD20. (E) To test the raft localization property of CD20 upon STIM1 binding, RAMOS cells transfected with scramble or siSTIM1 were treated with rituximab or obinutuzumab, then their binding amount were quantified by the FITC conjugated secondary antibodies. In siSTIM1 treated condition, the insolubilized CD20 were increased.

the efficacy of direct binding mediated cell death via obinutuzumab.

9. External Ca^{2+} is essential for the homotypic adhesion, but not required for direct binding mediated cell death by obinutuzumab. It is dependent on the external concentration of Mg^{2+}

In some of previous studies, HA (homotypic adhesion) induced by obinutuzumab is the main cause of obinutuzumab induced DCD (direct cell death). To observe the Ca^{2+} dependency of the HA and DCD by obinutuzumab, HA and DCD was tested the in 2mM Ca^{2+} or Ca^{2+} free external solutions. As expected, obinutuzumab induced HA was only occurred in 2mM Ca^{2+} external solution, which implied that homotypic adhesion by obinutuzumab is dependent on extracellular Ca^{2+}. (Fig. 9A). But unexpectedly, DCD was not affected by extracellular Ca^{2+} concentration, even more DCD seems to be happened in Ca^{2+} free external solution than 2mM Ca^{2+} condition (Fig. 9B). Since DCD was not affected by Ca^{2+}, I searched which ion is related with DCD by obinutuzumab. Among various ion, Mg^{2+} concentration exhibit potential effect on DCD, and then Mg^{2+} concentration was variated in external solution. In normal Mg^{2+} range, 1.5 mM Mg^{2+}, obinutuzumab had a superior effect on DCD. But the degree of DCD is not different between rituximab and obinutuzumab in 0 mM Mg^{2+}. In addition, when the magnesium concentration is increased up to 5mM and 10mM, the rate of DCD is also similar between rituximab and obinutuzumab. These data indicated that the typical DCD induced by obinutuzumab is totally dependent on the Mg^{2+} concentration in external solution, which might imply that the Mg^{2+} permeability through CD20 is the main cause of the DCD via obinutuzumab binding in RAMOS cells (Fig. 9C).

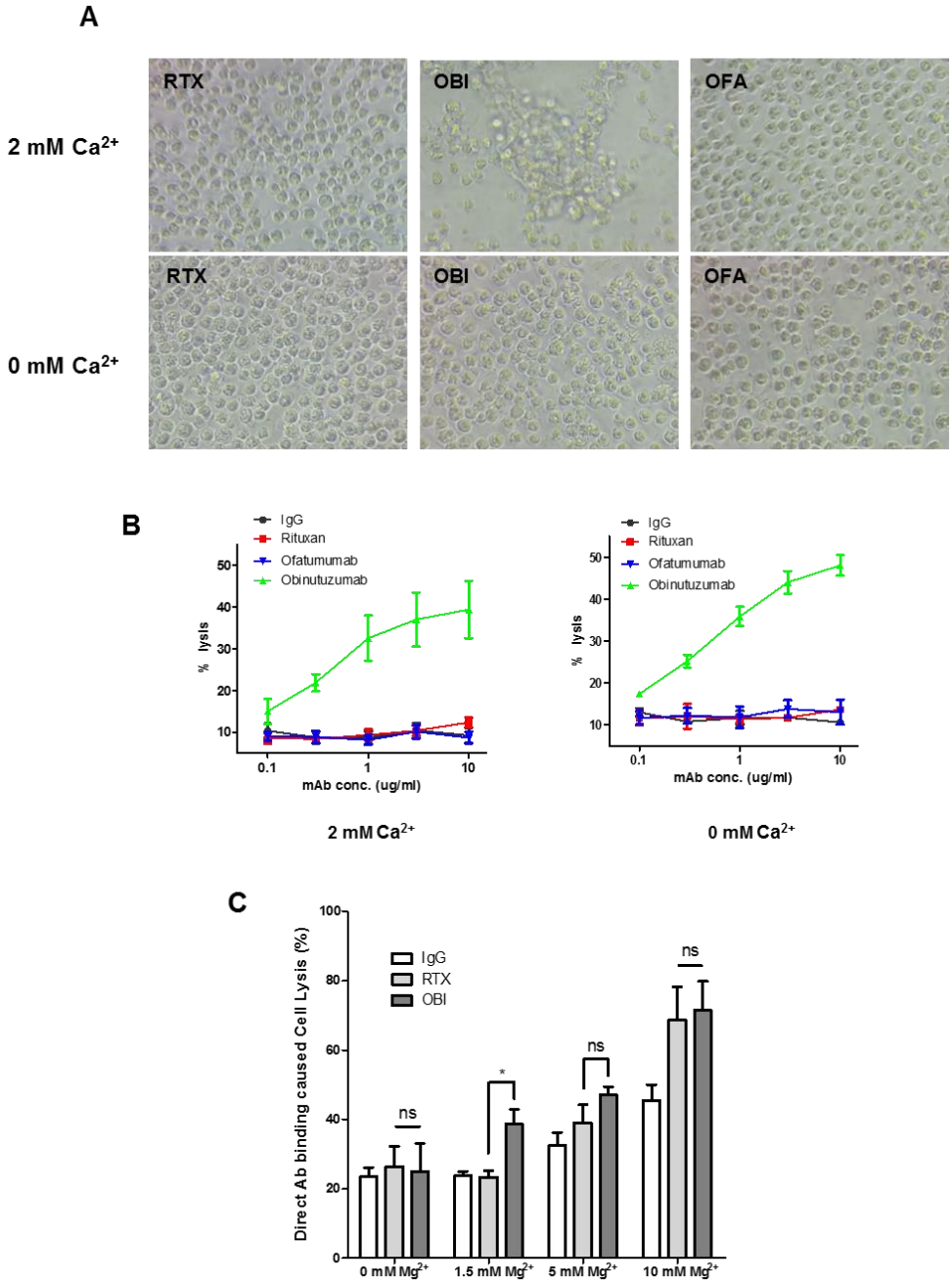

Figure 9. External Ca^{2+} is essential for the homotypic adhesion, but not required for direct binding mediated cell death by obinutuzumab. (A) To determine the

Ca^{2+} dependency of the obinutuzumab induced phenomenon, homotypic adhesion was observed in 2 mM Ca^{2+} and Ca^{2+} free solution. rituximab and ofatumumab did not showed any homotypic cell aggregation in both solution, but obinutuzumab showed cell aggregation only in 2 mM Ca^{2+} solution. (B) Direct binding mediated cell death were tested is a various concentration of rituximab, obinutuzumab, and ofatumumab in 2 mM Ca^{2+} or Ca^{2+} free external solution. In both solution, rituximab and ofatumumab did not showed any cell death via binding, but only obinutuzumab showed direct cell death in both solutions. (C) Mg^{2+} dependent direct cell death mediated by obinutuzumab binding. To test whether Mg^{2+} concentration in external solution is related with obinutuzumab induced direct binding mediated cell death in RAMOS cells, Mg^{2+} free, 1.5mM Mg^{2+}, 5 mM Mg^{2+}, 10 mM Mg^{2+} and bafilomycin treated in 1.5 mM Mg^{2+} were used then antibodies were treated for 12 hr. The cell lysis % were depicted as a graph. *p<0.05 and ns, not significant. 4 independent experiment summarized in graph.

IV. DISCUSSION

In spite of previous intensive study, as yet no clear function or ligand has been revealed for CD20, and only clinical effects were studied well. Store operated calcium influx was observed in cells transfected with CD20 at 2003, but there is still controversy as to whether CD20 itself has a channel function.

In this study, the pore function of CD20 as a SOC channel was studied by examining the molecular interactions with stim1 and identified how the pore function of CD20 effects on the function of anti-CD20 antibodies, rituximab and obinutuzumab.

To understand the pore function of CD20, the interaction of CD20 with STIM1 was observed in heterologous expression system and RAMOS cells. And I found their enhanced interaction in store depletion, and constitutive activation form of STIM1 which proves that the CD20 is a store operated channel. In addition, the CD20 channel activity regulated by STIM1 is dependent on Orai1, which implied that CD20 involved in the protein complexes with orai1 and STIM1 to function as SOC channel.

Next, it should be noted that the Ca^{2+} influx induced by antibody binding. In previous study, rituximab was crosslinked with a second polyclonal antibody to generate a calcium flux in Ramos cell. But in our image based data, external Ca^{2+} influx was observed even without crosslinking in Ramos cell. Considering the same phenomenon appears in cells expressing high level of cd20 such as Daudi or SU-DHL-4[23], this is thought to be caused by the difference in the expression level of CD20 and CD20 expression may change depending on the culture environment.

Meanwhile, the Ca^{2+} influx induced by binding of obinutuzumab on CD20 was enhanced by STIM1 co-expression. Moreover, the binding affinity to obinutuzumab was attenuated by knock-down of STIM1 expression using siRNA for STIM1. Besides, non-raft localized CD20 were decreased by siSTIM1 treated RAMOS cells. These results support that the configuration of CD20 is largely divided into two forms (lipid raft form and non-lipid raft form) and each function will be different. In addition, obinutuzumab causes the change of CD20 configuration to migrate into the non-lipid

raft region, which might activate the pore function of CD20 and induce the typical cell death. Thus, these all data demonstrated that the CD20 configuration regulated by STIM1 is effects on the function of anti-CD20 antibodies, especially obinutuzumab.

Next, focusing on the physiological function of the antibody, the homotypic adhesion and direct cell death induced by obinutuzumab. HA and DCD, which is a typical phenomenon that occur only by obinutuzumab, were expected to be Ca^{2+} dependent phenomenon and HA is known to as a main cause of DCD in previous report.[9,18] However, HA is occurred in a Ca^{2+} dependent manner, but external Ca^{2+} did not effect on the DCD. So HA is considered to be a secondary event occurring after DCD. Further study using latrunculin or actinomycine, the actin immobilizing drug, will be revealed that the DCD process has priority over HA.

In our study, even if the direct cell death induced by obinutuzumab is not dependent on the external Ca^{2+} concentration, I cannot not exclude that the pore function of CD20 is required for DCD by the obinutuzumab, because the Mg^{2+} concentration in external solution is critical for the DCD. At present, I don't know why the Mg^{2+} in external solution is required for the DCD by obinutuzumab. Further study showing the Mg^{2+} influx changes by obinutuzumab will clarify the Mg^{2+} pore function of CD20 and its relation of DCD by obinutuzumab. In a previous study, there was a report that DCD might be associated with the explosion of lysosomes. [9,19,20] The lysosome has a pH control mechanism regulated Mg^{2+}, therefore I expect that the Mg^{2+} may be involved in DCD process.[21,22]

In conclusion, the possibility that CD20 enact as a pore and that could influence function of antibody. Even if external Ca^{2+} didn't affect the DCD by obinutuzumab, there are the possibility that influx of other ions such as Mg^{2+} through CD20 could regulate the DCD by obinutuzumab.

V. CONCLUSION

In this study, I demonstrate that CD20 enact as a pore and CD20 involved in a protein complexes with Orai1 and STIM1 to function as SOC channel. This configuration of CD20 being regulated by STIM1 contributes to the efficacy of anti-CD20 antibodies. Especially, obinutuzumab causes the change of CD20 configuration to migrate into the non-lipid raft region and activate the pore function of CD20. Perhaps, the permeability of Mg^{2+} through CD20 might be involved in DCD by obinutuzumab.

REFERENCES

1. Tedder TF, Klejman G, Disteche CM, Adler DA, Schlossman SF, Saito H. Cloning of a complementary DNA encoding a new mouse B lymphocyte differentiation antigen, homologous to the human B1 (CD20) antigen, and localization of the gene to chromosome 19. J Immunol 1988;141:4388-94.

2. Walport M, Murphy K, Janeway C, Travers PJ. Janeway's Immunobiology (7th ed). 2008.

3. Polyak MJ, Tailor SH, Deans JP. Identification of a cytoplasmic region of CD20 required for its redistribution to a detergent-insoluble membrane compartment. J Immunol 1998;161:3242-8.

4. Janas E, Priest R, Wilde JI, White JH, Malhotra R. rituximab (anti-CD20 antibody)-induced translocation of CD20 into lipid rafts is crucial for calcium influx and apoptosis. Clin Exp Immunol 2005;139:439-46.

5. Mossner E, Brunker P, Moser S, Puntener U, Schmidt C, Herter S, et al. Increasing the efficacy of CD20 antibody therapy through the engineering of a new type II anti-CD20 antibody with enhanced direct and immune effector cell-mediated B-cell cytotoxicity. Blood 2010;115:4393-402.

6. Kern DJ, James BR, Blackwell S, Gassner C, Klein C, Weiner GJ. GA101 induces NK-cell activation and antibody-dependent cellular cytotoxicity more effectively than rituximab when complement is present. Leuk Lymphoma 2013;54:2500-5.

7. Beers SA, French RR, Chan HT, Lim SH, Jarrett TC, Vidal RM, et al. Antigenic modulation limits the efficacy of anti-CD20 antibodies: implications for antibody selection. Blood 2010;115:5191-201.

8. Klein C, Lammens A, Schafer W, Georges G, Schwaiger M, Mossner E, et al. Epitope interactions of monoclonal antibodies targeting CD20 and their relationship to functional properties. MAbs 2013;5:22-33.

9. Alduaij W, Ivanov A, Honeychurch J, Cheadle EJ, Potluri S, Lim SH, et al. Novel type II anti-CD20 monoclonal antibody (GA101) evokes

homotypic adhesion and actin-dependent, lysosome-mediated cell death in B-cell malignancies. Blood 2011;117:4519-29.

10. Li H, Ayer LM, Lytton J, Deans JP. Store-operated cation entry mediated by CD20 in membrane rafts. J Biol Chem 2003;278:42427-34.

11. Vacher P, Vacher AM, Pineau R, Latour S, Soubeyran I, Pangault C, et al. Localized Store-Operated Calcium Influx Represses CD95-Dependent Apoptotic Effects of rituximab in Non-Hodgkin B Lymphomas. J Immunol 2015;195:2207-15.

12. Lewis RS. The molecular choreography of a store-operated calcium channel. Nature 2007;446:284-7.

13. Parker NJ, Begley CG, Smith PJ, Fox RM. Molecular cloning of a novel human gene (D11S4896E) at chromosomal region 11p15.5. Genomics 1996;37:253-6.

14. Williams RT, Manji SS, Parker NJ, Hancock MS, Van Stekelenburg L, Eid JP, et al. Identification and characterization of the STIM (stromal interaction molecule) gene family: coding for a novel class of transmembrane proteins. Biochem J 2001;357:673-85.

15. Roos J, DiGregorio PJ, Yeromin AV, Ohlsen K, Lioudyno M, Zhang S, et al. STIM1, an essential and conserved component of store-operated Ca2+ channel function. J Cell Biol 2005;169:435-45.

16. Liou J, Kim ML, Heo WD, Jones JT, Myers JW, Ferrell JE, Jr., et al. STIM is a Ca^{2+} sensor essential for Ca^{2+}-store-depletion-triggered Ca^{2+} influx. Curr Biol 2005;15:1235-41.

17. Zhou Y, Srinivasan P, Razavi S, Seymour S, Meraner P, Gudlur A, et al. Initial activation of STIM1, the regulator of store-operated calcium entry. Nat Struct Mol Biol 2013;20:973-81.

18. Bologna L, Gotti E, Manganini M, Rambaldi A, Intermesoli T, Introna M, et al. Mechanism of action of type II, glycoengineered, anti-CD20 monoclonal antibody GA101 in B-chronic lymphocytic leukemia whole blood assays in comparison with rituximab and alemtuzumab. J Immunol 2011;186:3762-9.

19. Honeychurch J, Alduaij W, Azizyan M, Cheadle EJ, Pelicano H, Ivanov A, et al. Antibody-induced nonapoptotic cell death in human lymphoma and leukemia cells is mediated through a novel reactive oxygen species-dependent pathway. Blood 2012;119:3523-33.

20. Jak M, van Bochove GG, Reits EA, Kallemeijn WW, Tromp JM, Umana P, et al. CD40 stimulation sensitizes CLL cells to lysosomal cell death induction by type II anti-CD20 mAb GA101. Blood 2011;118:5178-88.

21. Jha A, Ahuja M, Patel S, Brailoiu E, Muallem S. Convergent regulation of the lysosomal two-pore channel-2 by Mg^{2+}, NAADP, $PI_{3,5}P_2$ and multiple protein kinases. Embo j 2014;33:501-11.

22. Miao Y, Li G, Zhang X, Xu H, Abraham SN. A TRP Channel Senses Lysosome Neutralization by Pathogens to Trigger Their Expulsion. Cell 2015;161:1306-19.

23. Walshe CA, Beers SA, French RR, Chan CH, Johnson PW, Packham GK, et al. Induction of cytosolic calcium flux by CD20 is dependent upon B Cell antigen receptor signaling. J Biol Chem 2008;283:16971-84.

ABSTRACT (in Korean)

CD20의 칼슘통로활성이 Rituximab과 Obinutuzumab의 효능에 미치는 영향

<지도교수 김 주 영>

연세대학교 대학원 의과학과

허 운

CD20은 세포막을 4번 통과하는 단백으로서, 비호치킨성 림프종의 치료제와 만성관절염의 치료제의 표적이 되는 단백이다. CD20이 SOC 통로특성을 가지고 있음은 기존의 여러 연구에서 보고하였지만, CD20이 SOC 통로라는 결론을 확실히 내릴 수 있는 STIM1과의 결합 여부에 대한 보고는 전무하다.

이를 바탕으로 본 논문에서는 1) CD20의 세포막 통로로서의 특성 파악과 2) SOC 기전을 통한 칼슘 신호가 각 항체에 대한 역가나 특성을 결정하는데 어떠한 영향을 미칠 것인지 규명하고자 하였다.

CD20와 STIM1의 단백상호작용 확인한 결과, CD20이 STIM1과 상호작용은 세포내 칼슘저장고 고갈에 의해서 증가할 뿐 아니라 Orai1에 의존적인 것이 확인되었다. 이는 CD20이 단독으로 세포막 통로로서 작용한다기보다 STIM1과 Orai1이 이루는 단백복합체에 참여한다

항체를 생산함에 있어선 lentivirus system을 이용하였으며 항체의 생산, 정제 과정, 정제 후 과정에서 정상적인 항체가 만들어졌는지 확인하였다. 그 결과 항원 특이성, 각 항체의 특이적 기능 등이 알려진 바와 일치하였다.

생산된 항체를 각각 CD20가 과 발현 된 HEK293T 세포에 처리한 결과 rituximab 과 obinutuzumab 모두 외부로부터의 칼슘 유입을 보였으나 STIM1과의 단백 상호 작용은 항체의 종류에 따라 다른 영향을 미쳤다. rituximab 의 경우, CD20와 STIM1의 결합으로 인한 영향이 미미했던 반면에, obinutuzumab 의 경우 항원인 CD20에 결합하는 능력과 외부로부터 들어오는 칼슘의 양이 모두 유의하게 증가하였다. 이는 STIM1과 상호작용하는 CD20 세포막 통로적 특징이 항체의 기능에 선택적으로 영향을 줄 수 있음을 시사한다.

obinutuzumab 특이적인 세포 동형성 접착 현상(homotypic adhesion)과 직접적 세포사멸 기전(direct cell death)이 외부 칼슘 농도에 의존적인지 살펴본 결과 흥미롭게도, 세포 동형성 접착의 경우 외부 칼슘 농도의존적으로 일어나는 반면 직접적 항체 결합에 의한 세포 사멸의 경우 외부 칼슘 농도에 상관 없이 일어남을 보였다. obinutuzumab 에 의한 직접적 항체 결합에 의한 세포 사멸이 칼슘 이외의 이온의 연관성을 살펴본 결과 세포 외부의 마그네슘 농도가 obinutuzumab 결합의존적 세포사멸에 중요함을 발견하였다.

결론적으로 본 연구는 CD20이 STIM1과 Orai1의존적으로 기능하는 세포내 칼슘저장고 의존적 칼슘 통로이며 이러한 CD20의 칼슘통로로서의 특성은 각 항체 rituximab 과 obinutuzumab 의 결합에 의해서 활성화됨을 규명하였다. 특히 obinutuzumab 에 의한 항체 결합-의존적 세포사멸은 CD20의 Mg^{2+}통과 기능과 연관되어 있을 것으로 생각한다.

핵심되는 말: CD20, STIM1, SOCE, 칼슘, 마그네슘, rituximab, obinutuzumab.

PUBLICATION LIST